First-principles study of the electronic structure of PbF_2 in the cubic, orthorhombic, and hexagonal phases

2004 J. Phys.: Condens. Matter 16 3081

(http://iopscience.iop.org/0953-8984/16/18/009)

INSTITUTE OF PHYSICS PUBLISHING JOURNAL OF PHYSICS: CONDENSED MATTER

J. Phys.: Condens. Matter **16** (2004) 3081–3088 PII: S0953-8984(04)75127-9

First-principles study of the electronic structure of PbF_2 in the cubic, orthorhombic, and hexagonal phases

Huitian Jiang[1], **Roberto Orlando**[2], **Miguel A Blanco**[3] **and Ravindra Pandey**[1]

[1] Department of Physics, Michigan Technological University, Houghton, MI 49931, USA
[2] Dipartimento di Scienze e Tecnologie Avanzate, Università del Piemonte Orientale, C. so Borsalino 54, I-15100 Alessandria, Italy
[3] Departamento de Química Física y Analítica, Universidad de Oviedo, 33006-Oviedo, Spain

Received 31 December 2003
Published 23 April 2004
Online at stacks.iop.org/JPhysCM/16/3081
DOI: 10.1088/0953-8984/16/18/009

Abstract

The results of electronic structure calculations for PbF_2 in ambient and high-pressure phases are reported here. We employ the linear combination of atomic orbital-density functional theory approximation using the CRYSTAL program package whose capabilities were expanded to include the so-called soft-core pseudopotentials with higher-order components (e.g. d, f, and g) of the angular momentum terms for heavier atoms in the periodic table. The band structure and density of states of the cubic, orthorhombic, and hexagonal phases were calculated. A direct band gap at X is predicted for the cubic phase, whereas an indirect band gap is predicted for the high-pressure phases. The density of states reveals hybridization features involving Pb s and F p orbitals in the upper valence band of PbF_2.

1. Introduction

Cubic lead fluoride (β-PbF_2) is a well-known fast ionic conductor at high temperatures [1]. Recently, it has attracted renewed interest as a promising host material for scintillating detectors for detecting high-energy particles with energy exceeding a gigaelectronvolt [2–4]. This is due to the fact that PbF_2 satisfies most of the requirements for a scintillating detector, namely short radiation length, high light yield, short decay time, and good radiation hardness. Furthermore, single crystals of PbF_2 can be grown by a relatively inexpensive crystal growth process, thereby providing economical incentives for making scintillating detectors [5, 6].

A faint scintillating light in the orthorhombic (α-) phase of polycrystalline PbF_2 was observed at room temperature, which was stimulated by synchrotron x-rays [2]. It is generally believed that scintillation in PbF_2 is mainly associated with rare-earth dopants, unlike the case for the well-known barium fluoride (BaF_2) where the scintillation mechanism is attributed to the intrinsic luminescence of the host. The crystalline lattice of PbF_2 facilitates a dense

and ideal structure frame in which the scintillating rare-earth atoms are embedded. For Gd-doped cubic PbF_2 at room temperature, Shen and co-workers have reported fast luminescent components at 277.5 and 312.4 nm, with a light yield of >6.2 p.e. MeV^{-1} and a decay time of <30 ns [3, 7]. The observed light output and decay were found to satisfy the requirements of γ-ray scintillating detectors with good energy resolution and high counting rate.

At low pressures, PbF_2 is found to exist in two structural phases, namely orthorhombic (α) and cubic (β). Although the cubic phase is the most stable in ambient conditions, the orthorhombic phase is stable at high pressure and low temperature. The cubic phase undergoes a phase transition at about 0.4 GPa to the orthorhombic phase and reverts back to the cubic phase at higher temperatures. The orthorhombic phase is metastable at zero pressure for temperatures <610 K [8]. Above 15 GPa, a new high-pressure phase of PbF_2 was observed [9, 10]. Podsiadlo and Matuszewski [9] have reported it to have hexagonal symmetry, tentatively assigned as P6, with lattice parameters of $a = 10.2746(6)$ Å and $c = 7.970(5)$ Å. On the other hand, Lorenzana *et al* [10] have proposed the structure to be monoclinic, assuming the existence of some unresolved peaks in their Raman experiments. This is in contrast to the results of first-principles calculations based on the *ab initio* perturbed ion (*ai*PI) method [11], where the post-cotunnite phase is the hexagonal, Ni_2In-like, $B8_b$ phase. The hexagonal phase was found to be stable relative to the orthorhombic phase at 16.4 GPa [11].

Excitonic transitions in orthorhombic and cubic PbF_2 were reported to have similar features suggesting a similarity in the electronic structures of the two phases [12]. Specifically, the lowest excitonic transition at 5.7 eV was observed in both phases. Above 6 eV, two prominent peaks were observed. In orthorhombic (cubic) PbF_2, the peaks were at 6.25 (6.51) and 8.45 (8.58) eV. On the other hand, the photoelectron spectroscopy results have suggested the valence bands in cubic PbF_2 to be composed of lead 6s and fluorine 2p orbitals [13, 14]. Although band structure calculations differ from each other in describing the topology of the valence bands in the Brillouin zone, they agree in predicting the top of the valence band to be a mixture of lead 6s and fluorine 2p orbitals in cubic PbF_2 [15–17]. This is in contrast to the case for other ionic materials with the fluorite structure (e.g. BaF_2) where the lowest excitonic transition is mainly associated with transitions from anion p states to cation s states. It is to be noted here that a detailed understanding of the electronic properties of the host material is a necessary requirement for understanding the nature of the scintillating mechanism [7]. For example, the estimate of the intrinsic absorption edge of β-PbF_2 has shifted about 50 nm in about 20 years of experimental studies [3, 7, 18] suggesting a necessity for band structure calculations using state-of-the-art methods. On the other hand, the orthorhombic and hexagonal phases of PbF_2 have not yet been subject to any band structure calculations.

In this paper, we report the results of band structure calculations on the orthorhombic and hexagonal phases of PbF_2, for the first time, together with a more accurate and detailed band structure of the cubic PbF_2. Calculations are based on density functional theory using the CRYSTAL program package [19]. The CRYSTAL program was modified to accept d, f, and g terms in the effective core pseudopotential (ECP) description of heavier atoms, such as Pb. With this modification, calculations for all elements in the periodic table involving ECPs has become possible in the CRYSTAL program. The rest of the paper is organized as follows. In section 2, we briefly describe the computational techniques used in this work. Results and discussion of the electronic properties including the band structure and density of states will be presented in section 3 and a summary of the work will be given in section 4.

2. Methodology

Electronic structure calculations based on density functional theory (DFT) were performed in the framework of the periodic linear combination of atomic orbitals (LCAO) approximation. In

the LCAO DFT approximation, a linear combination of Gaussian orbitals is used to construct a localized atomic basis from which Bloch functions are constructed by a further linear combination with plane-wave phase factors. We note here that relativistic corrections for core electrons, which are important for heavier atoms such as lead, are not yet included in CRYSTAL for total energy calculations. However, one can now perform CRYSTAL calculations in which relativistic effects are taken into account in the definition of the ECPs for heavy atoms.

In the present study, calculations were performed with the new ECP module [20] developed by us for the CRYSTAL program package. This development work on CRYSTAL was mainly based on the analytical method proposed by McMurchie and Davidson [21] for ECPs fitted to Gaussian basis sets, which relies on the transformation of three-centre integrals into one-centre integrals. The ECP contribution to the orbital interactions generates two types of integral, referred to as type I and II, which can be factorized into a radial and an angular part. The integrals can be evaluated with the help of recursive relations for the modified Bessel functions and real spherical harmonics. However, no general analytical formula is available for the calculation of the radial part of type II integrals, where the difficulty is due to the appearance of projection operators. In our implementation we followed the suggestion by Skylaris *et al* [22] who have shown that numerical integration represents a valid and efficient alternative choice for the radial part of type II integrals, particularly when the log 3 quadrature scheme is used [23]. This technique of generating a radial grid of points is suitable for the evaluation of integrals involving Gaussian functions and allows an efficient gradual improvement of the grid to reach the required level of accuracy. As regards the problem of the infinite sums appearing in the evaluation of the ECP contributions in CRYSTAL, they are truncated on the basis of suitable overlap criteria.

The atomic number of lead is 82 and its electronic configuration can be represented as $[Xe]4f^{14}5d^{10}6s^26p^2$. In this work, the inner shells consisting of 68 electrons ($[Xe]4f^{14}$) were represented by the CRENBL effective core potential [24], which is constructed from a series of Gaussian-like orbitals. Furthermore, it is assumed that electrons in the outer shells of lead (i.e. 5d, 6s, and 6p orbitals) can provide a reliable and accurate description of the salient features of the band structure of PbF_2. A Gaussian basis set of (21/21/21) with 2s-, 2p-, and 2d-type shells was used to represent electrons in the outer shells of Pb. The basis set for fluorine, which consists of 4s- and 3p-type shells (i.e. a 7311/311 set), was taken from the LCAO DFT study of the electronic structure of BaF_2 [25], where additional diffuse and polarization functions of s- and p-type shells were added to the F^- ionic basis set. The exponents of the outermost functions in both lead and fluorine basis sets were optimized at the experimental geometry of the cubic PbF_2 by performing total energy calculations. The basis sets and ECPs of lead and fluorine used in this study can be obtained from the authors (pandey@mtu.edu).

It is well known that calculations based on density functional theory underestimate the band gap, while Hartree–Fock calculations generally overestimate the gap. However, it has recently been reported that DFT calculations employing the B3LYP exchange and correlation functional form can yield band gaps which are in very good agreement with the corresponding experimental values [26]. In the present work, we therefore use the B3LYP functional form for DFT calculations on PbF_2. We set the tolerance on the total energy convergence in the iterative solution of the Kohn–Sham equations to be 10^{-6} Hartree and a grid of 300 k-points was used in the irreducible Brillouin zone for integration in the reciprocal space.

3. Results: structural properties

We begin with cubic PbF_2 for which both experimental and previous theoretical results are available for benchmarking the model elements, e.g. ECPs for Pb used in the LCAO DFT calculations for orthorhombic and hexagonal phases.

The cubic phase has only one free parameter, a, the length of the cell, since all ions are occupying fixed special Wyckoff positions. The calculated potential energy surface for the cubic phase was fitted to the equation of state of Vinet *et al* [27, 28] to obtain equilibrium values for the lattice constant a, the bulk modulus (B), and its pressure derivative (B') at zero pressure. The calculated values of a, B, and B' are 5.98 Å, 60.36 GPa, and 4.84, respectively.

Previously, Hartree–Fock calculations [16] reported values of 5.89 Å, 87.5 GPa, and 4.47 for a, B, and B', respectively. *ai*PI calculations including LYP correlation, on the other hand, yield values of 5.98 Å, 56 GPa, and 4.90 for a, B, and B', respectively [11].

The experimental value of a is reported to be 5.94 Å [29, 30]. The agreement between the experimental and DFT, Hartree–Fock and DFT–*ai*PI values for a in cubic PbF_2 is therefore excellent. However, there are two sets of experimental values for B. The bulk modulus computed from elastic measurements is reported to be 60.5 GPa [31], while that computed from the equation of state [32] is found to be 60.6 GPa. On the other hand, White [33] has reported the value of B to be 70.6 GPa. Both the present study and *ai*PI calculations [11] therefore support a value of about 60 GPa for the bulk modulus of the cubic PbF_2.

The orthorhombic phase has two independent variables (i.e. b/a and c/a) for a fixed unit cell volume [34]. Its unit cell has six internal parameters (i.e. x_{Pb}, z_{Pb}, x_{F_1}, z_{F_1}, x_{F_2}, z_{F_2}) that need to be optimized. Total energy optimization of the orthorhombic phase therefore requires the optimization of six internal variables together with b/a and c/a for each point in the potential energy curve. On the other hand, the high-pressure hexagonal phase can be characterized by two independent variables (i.e. a and c/a) for a fixed unit cell volume [34].

In this study, we have taken the rather simple approach of taking the optimized structural coordinates from the results of *ai*PI calculations on the orthorhombic and hexagonal phases [11], instead of performing extensive structural optimization of these phases of PbF_2. This approach is justified due to the fact that CRYSTAL and *ai*PI methods using DFT correlation have previously been shown to predict similar structural properties for a wide variety of materials. The present approach would therefore provide significant savings of computational resources. Furthermore, the focus of the present study is on providing details of the band structure of the orthorhombic and hexagonal phases whose structural properties have been characterized very well in the previous *ai*PI study. It is to be noted here that the *ai*PI method cannot provide details of the band structure of a given material.

The *ai*PI values of the molar volume of the orthorhombic and hexagonal phases of PbF_2 are 29.60 $cm^3\ mol^{-1}$ (with $a = 6.56$ Å, $b = 3.93$ Å, and $c = 7.62$ Å) and 28.18 $cm^3\ mol^{-1}$ (with $a = 4.24$ Å and $c = 6.00$ Å), respectively. For the orthorhombic phase, the values of the internal parameter taken from *ai*PI calculations are as follows: $x_{Pb} = 0.245$, $z_{Pb} = 0.114$, $x_{F_1} = 0.356$, $z_{F_1} = 0.428$, $x_{F_2} = 0.973$, and $z_{F_2} = 0.674$.

4. Results: electronic properties

The valence and conduction band structures of the ambient and high-pressure phases of PbF_2 considered in this study are displayed in figures 1–3. For the cubic phase, the DFT–CRYSTAL band structure is very similar to the previously reported HF–CRYSTAL band structure, except the value of the band gap which is predicted to be 6.3 eV in the present study. The excitonic spectrum [12] of cubic PbF_2 reports the first peak to be about 5.7 eV. Assuming the exciton binding energy to be a few tenths of an electronvolt, the DFT–CRYSTAL value of the band gap obtained using the B3LYP functional form turns out to be in very good agreement with the (extrapolated) measured value of about 5.9 eV. It is to be noted here that DFT calculations using the BPW functional form underestimate the band gap, with a value of 4.2 eV. The B3LYP functional form for DFT calculations does therefore provide a better agreement with

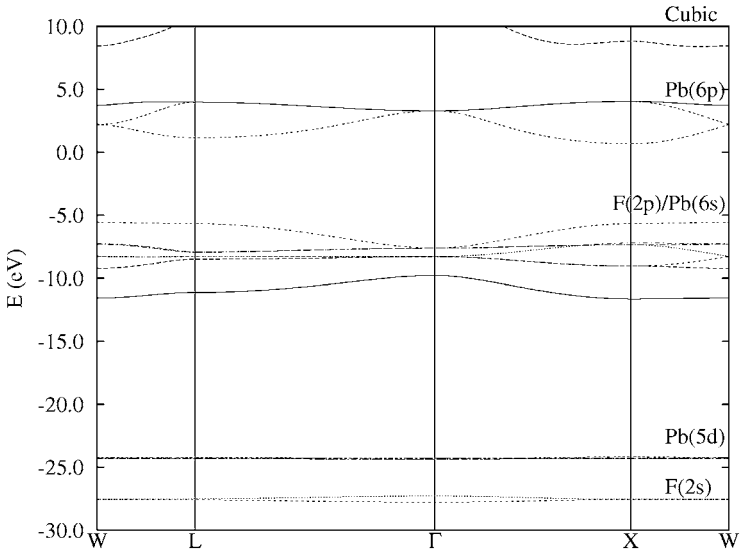

Figure 1. The band structure of β-PbF_2 (cubic). The Pb(6p) band forms the bottom of the conduction band. Featured k-points are: W $\langle\frac{1}{2}\frac{1}{4}\frac{3}{4}\rangle$, L $\langle\bar{\frac{1}{2}}\frac{1}{2}\frac{1}{2}\rangle$, Γ $\langle 000\rangle$, and X $\langle\frac{1}{2}0\frac{1}{2}\rangle$.

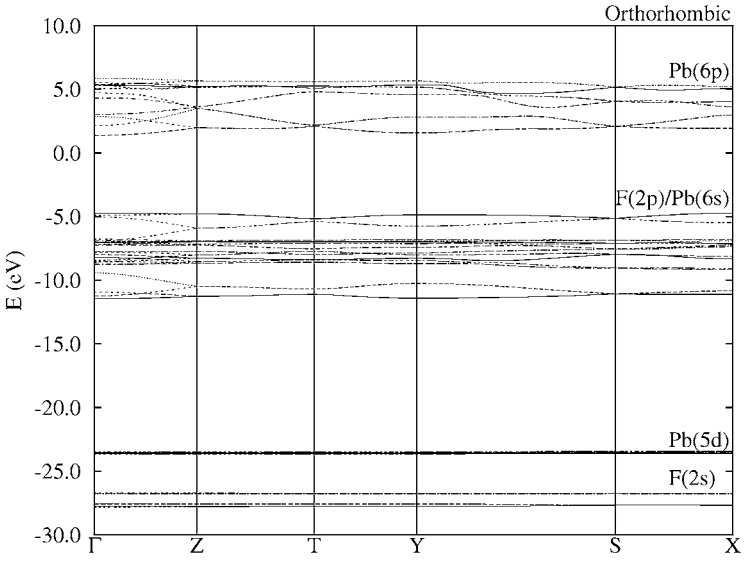

Figure 2. The band structure of α-PbF_2 (orthorhombic). The Pb(6p) band forms the bottom of the conduction band. Featured k-points are: Γ $\langle 000\rangle$, Z $\langle 00\frac{1}{2}\rangle$, T $\langle\bar{\frac{1}{2}}0\frac{1}{2}\rangle$, Y $\langle\bar{\frac{1}{2}}00\rangle$, S $\langle\bar{\frac{1}{2}}\frac{1}{2}0\rangle$, and X $\langle 0\frac{1}{2}0\rangle$.

the experimental value of the band gap in PbF_2, as also reported in several other cases [26]. We note that the spin–orbit splittings of the valence and conduction bands are not taken into account in the present study.

The topological nature of the valence band in PbF_2 is found to be significantly different from the one observed in alkaline-earth fluorides, such as BaF_2. In PbF_2, the upper valence band has contributions from both fluorine 2p and lead 6s orbitals. This cationic–anionic s/p-type admixture yields the maximum of the valence band as being away from the Γ point in all the phases of PbF_2 considered here. In the cubic phase, the maximum is at X which is about 1.95 eV higher in energy relative to Γ. The L point and X point are almost degenerate in the cubic phase. In the orthorhombic phase, the top of the valence band does not show significant dispersion along the $\langle 0\frac{1}{2}0\rangle$ symmetry direction making X a maximum by only 0.014 eV relative

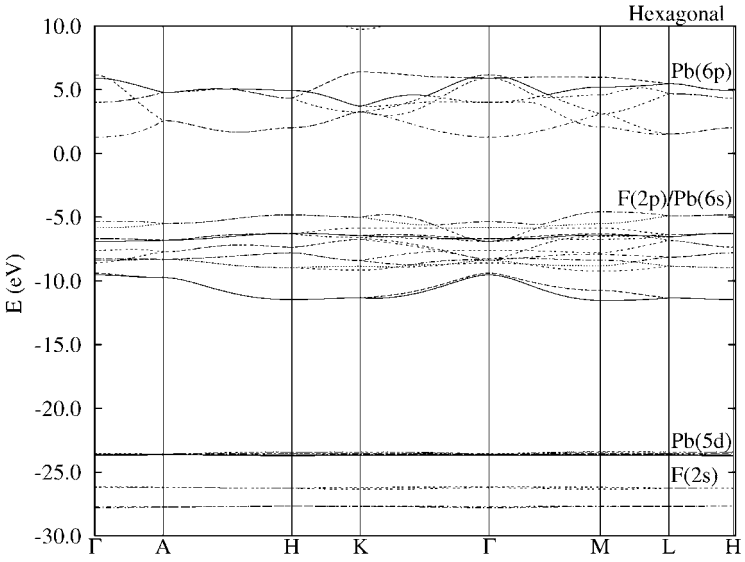

Figure 3. The band structure of γ-PbF_2 (hexagonal). The Pb(6p) band forms the bottom of the conduction band. Featured k-points are: Γ $\langle 000\rangle$, A $\langle 00\frac{1}{2}\rangle$, H $\langle \bar{\frac{1}{3}}\,\frac{2}{3}\,\frac{1}{2}\rangle$, K $\langle \bar{\frac{1}{3}}\,\frac{2}{3}0\rangle$, and M $\langle 0\frac{1}{2}0\rangle$, L $\langle 0\bar{\frac{1}{2}}\,\frac{1}{2}\rangle$.

Table 1. Band gaps, valence bandwidths, and the location of the Pb(d) band with reference to the top of the valence band in PbF_2. The unit is eV.

	Cubic		Orthorhombic		Hexagonal	
Band gap	Γ	11.65	Γ	6.12	Γ	6.64
(direct)	X	6.30	X	6.68	M	6.66
	L	6.82	Y	6.43	L	6.43
Band gap	X–Γ	9.07	X–Γ	6.10	M–Γ	5.87
(indirect)	X–L	6.76	X–Y	6.30	M–L	6.12
Bandwidth	Upper valence band	6.65		6.78		6.93
	Pb(5d) band	0.21		0.23		0.31
Band location	Pb(5d) band	18.8		18.8		18.7

to Γ. In the hexagonal phase, the dispersion along $\langle 0\frac{1}{2}0\rangle$ becomes more pronounced with the maximum at M 0.76 eV higher than that at Γ.

In contrast to valence bands, conduction bands in PbF_2 show significant variation in their topology in going from cubic to orthorhombic to hexagonal. The minimum of the conduction band is mainly composed of lead 6p orbitals, and is at X in the cubic phase. However, it shifts to Γ in both orthorhombic and hexagonal phases. In the high-symmetry cubic phase, it therefore appears that s–p hybridization between lead and fluorine orbitals pushes Pb(6p) orbitals (in the conduction band) to higher energy at Γ than those in the low-symmetry phases (i.e. orthorhombic and hexagonal) of PbF_2. The resulting minimum energy gaps are 6.3 eV ($X^v \rightarrow X^c$), 6.10 eV ($X^v \rightarrow \Gamma^c$), and 5.87 eV ($M^v \rightarrow \Gamma^c$) in the cubic, orthorhombic, and hexagonal phases, respectively. Table 1 collects values of the energy gap at various symmetry points in the Brillouin zone for the phases considered here. The DFT–CRYSTAL calculations, therefore, predict PbF_2 in the orthorhombic and hexagonal phases to be an indirect gap material, in contrast to the predicted direct gap for cubic PbF_2.

The total density of states (DOS) for the cubic, orthorhombic, and hexagonal phases is displayed in figure 4. The calculated DOS agrees well with the HF–CRYSTAL calculations in identifying the peaks in the experimental photoemission spectrum [14] of cubic PbF_2. Analysis of the projected density of states identifies the peak associated with the top of the valence band

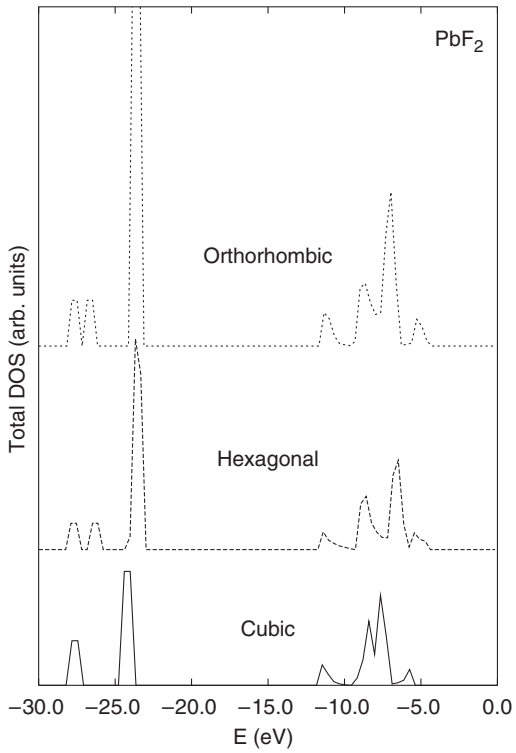

Figure 4. The total density of states of cubic, orthorhombic, and hexagonal PbF_2. It is shifted to reveal the features and is not normalized to the same number of atoms in the given unit cell.

as being due to Pb(6s) orbitals but that associated with the bottom of the conduction band as being due to Pb(6p) orbitals. In going from cubic to orthorhombic and hexagonal phases, the nature of the peaks does not change. However, the shape of the peak associated mainly with F(2p) orbitals changes due to the change in the symmetry of the fluorine lattice sites in the orthorhombic and hexagonal phases. In the cubic phase, the calculated width of the upper valence band turns out to be 6.7 eV as compared to the experimental value of about 7.0 eV and the HF value of 9.0 eV. In the orthorhombic and hexagonal phases, the width is about 6.8 and 6.9 eV, respectively.

Since Pb(5d) electrons are treated as a part of valence electrons in the present study, the DFT calculations can provide their location with respect to the top of the valence band. As shown in figure 1, the Pb(5d) band is atomic-like with a negligible dispersion appearing at about 18.8 eV below the top of the valence band. The location of the Pb(5d) band remains nearly the same in going from cubic to orthorhombic to the hexagonal phase.

The F(2s) band in cubic PbF_2 is located about 22.6 eV below the top of the valence band. Since there are two inequivalent fluorine atoms in both the low-symmetry orthorhombic and hexagonal PbF_2 phases, two distinct F(2s) bands with negligible dispersion appear in their band structures.

Mulliken population analysis indicates that the charges associated with Pb and F are +1.50 and -0.75, respectively, in the phases considered here and suggests the presence of a small contribution of covalency in the PbF_2 lattice.

5. Summary and conclusions

We utilize the new ECP package in the CRYSTAL program to conduct LCAO DFT calculations on PbF_2. The calculated results provide a very good description of its electronic structure in

ambient and high-pressure phases, predicting the cubic phase to be a direct gap material. The high-pressure orthorhombic and hexagonal phases are predicted to be indirect gap materials.

Acknowledgments

H Jiang and R Orlando thank V R Saunders for his useful suggestions about the implementation of the new ECP module in the CRYSTAL program. M A Blanco acknowledges financial support from the DGICyT, Projects BQU2000–0466 and BQU2003–06553.

References

[1] Samara G A 1979 Pressure and temperature dependences of the ionic conductivities of cubic and orthorhombic lead fluoride (PbF_2) *J. Phys. Chem. Solids* **40** 509–22
[2] Derenzo S E, Moses W W, Cahoon J L, Perera R C C and Litton J E 1990 Prospects for new inorganic scintillators *IEEE Trans. Nucl. Sci.* **37** 203–8
[3] Shen D Z, Ren G H, Deng Q and Yin Z W 1998 The scintillating property research of β-PbF_2 at room temperature *Sci. Sin.* E **28** 46–50
[4] Nessi-Tedadi F 1998 Overview of $PbWo_4$ calorimeter in cms *Nucl. Instrum. Methods Phys. Res.* A **408** 266–73
[5] Lempicki A and Wojtowicz A J 1994 Fundamental limitations of scintillators *J. Lumin.* **60/61** 942–7
[6] Lecoq P 1994 The high energy physics demand for a new generation of scintillators *J. Lumin.* **60/61** 948–55
[7] Ren G H 1998 The defects and dopant effect in β-PbF_2 crystal *PhD Thesis* Shanghai Institute of Ceramics
[8] Oberschmidt J and Lazarus D 1980 *Phys. Rev.* B **21** 2952
[9] Podsiadlo H and Matuszewski J 1994 *Mater. Chem. Phys.* **37** 397
[10] Lorenzana H E, Klepeis J E, Lipp M J, Evans W J, Radousky H B and van Schilfgaarde M 1997 *Phys. Rev.* B **56** 543
[11] Costales A, Blanco M A and Pandey R 2000 *Phys. Rev.* B **61** 11359
[12] Fujita M, Itoh M, Nakagawa H, Kitaura M and Alov D L 1998 Exciton transitions in orthorhombic and cubic PbF_2 *J. Phys. Soc. Japan* **67** 3320–1
[13] Tsujibayashi T, Watanabe M, Arimoto O, Itoh M, Kamada M and Asaka S 1999 Resonant enhancement effect on two-photon absorption due to excitons in alkaline-earth fluorides excited with synchrotron radiation and laser light *Phys. Rev.* B **60** R8442–5
[14] Chab V, Kowalski B and Orlowski B A 1986 *Solid State Commun.* **58** 667
[15] Velicky B and Masek J 1986 Electronic states in mixed $Cd_{1-x}Pb_xF_2$ crystals *Solid State Commun.* **58** 663–6
[16] Nizam M, Bouteiller Y, Silvi B, Pisani C, Causà M and Dovesi R 1988 *J. Phys. C: Solid State Phys.* **21** 5351–9
[17] Evarestov R A, Murin I V and Petrov A V 1984 *Sov. Phys.—Solid State* **26** 1563
[18] Nikl M and Polak K 1990 *Phys. Status Solidi* a **117** K89
[19] Saunders V R, Dovesi R, Roetti C, Causà M, Harrison N M, Orlando R and Zicovich-Wilson C M 1998 *CRYSTAL98 User's Manual* Torino
[20] Jiang H 2003 A theoretical study of fluoride scintillating crystals—methodology and application *PhD Thesis* Michigan Technological University
[21] McMurchie L E and Davidson E R 1981 *J. Comput. Phys.* **44** 289–301
[22] Skylaris C, Gagliardi L, Handy N C, Ioannou A G, Spencer S, Willetts A and Simper A M 1998 *Chem. Phys. Lett.* **296** 445–51
[23] Mura M E and Knowles P J 1996 *J. Chem. Phys.* **104** 9848
[24] Ross R B, Ermler W C and Christiansen P A 1990 *J. Chem. Phys.* **93** 6654
[25] Jiang H, Pandey R, Darrington C and Rérat M 2003 *J. Phys.: Condens. Matter* **15** 709–18
[26] Muscat J, Wander A and Harrison N M 2001 *Chem. Phys. Lett.* **342** 397–401
[27] Vinet P, Ferrante J and Smith J R 1989 *J. Phys.: Condens. Matter* **1** 1941
[28] Blanco M A, Francisco E and Luaña V 2003 *Comput. Phys. Commun.* **158** 57
[29] Simmons G and Warg H 1971 *Single Crystal Elastic Constants and Calculated Aggregated Properties: a Handbook* 2nd edn (Boston, MA: MIT Press)
[30] Jiang H, Costales A, Blanco M A, Gu M and Pandey R 2000 *Phys. Rev.* B **62** 803
[31] Catlow C R A, Comins J D, Germano F A, Harley R T and Hayes W 1978 *J. Phys. C: Solid State Phys.* **11** 3197
[32] Samara G A 1976 *Phys. Rev.* B **13** 4529
[33] White G K 1980 *J. Phys. C: Solid State Phys.* **13** 4905
[34] Wyckoff R W G 1960 *Crystal Structures* vol 2 (New York: Interscience)